行政院國家科學委員會專題研究計畫 成果報告

助聽器晶片及系統--子計畫七：微機電式聲學元件暨助聽器異質整合(3/3)
研究成果報告(完整版)

計 畫 類 別 ： 整合型
計 畫 編 號 ： NSC 98-2220-E-009-011-
執 行 期 間 ： 98 年 08 月 01 日至 99 年 07 月 31 日
執 行 單 位 ： 國立交通大學電子工程學系及電子研究所

計 畫 主 持 人 ： 鄭裕庭

計畫參與人員： 碩士班研究生-兼任助理人員：陳冠名
碩士班研究生-兼任助理人員：林耿宇
博士班研究生-兼任助理人員：陳永昌
博士班研究生-兼任助理人員：陳健章

報 告 附 件 ： 出席國際會議研究心得報告及發表論文

處 理 方 式 ： 本計畫可公開查詢

中 華 民 國 99 年 10 月 27 日

行政院國家科學委員會補助專題研究計畫成　果　報　告
■期中進度報告

助聽器晶片及系統-子計畫七：微機電式聲學元件暨助聽器異質整合(3/3)

計畫類別：□ 個別型計畫■國家型科技計畫(整合型)
計畫編號：NSC　98-2220-E-009-011-
執行期間：　98 年　8 月 1 日 至　99 年　7 月　31 日

計畫主持人：**國立交通大學電子工程系 鄭裕庭 教授**
共同主持人：
計畫參與人員：

成果報告類型(依經費核定清單規定繳交)：□精簡報告　■完整報告

本成果報告包括以下應繳交之附件：
□赴國外出差或研習心得報告一份
□赴大陸地區出差或研習心得報告一份
■出席國際學術會議心得報告及發表之論文各一份
□國際合作研究計畫國外研究報告書一份

處理方式：除產學合作研究計畫、提升產業技術及人才培育研究計畫、列管計畫及下列情形者外，得立即公開查詢
■涉及專利或其他智慧財產權，□一年■二年後可公開查詢

執行單位：**國立交通大學電子工程系**

中　華　民　國　99　年　10　月　20　日

微機電式聲學元件暨助聽器異質整合(3/3)

Design and Fabrication of MEMS Acoustic Devices and Technology Development of Heterogeneous Integration for Hearing Aid Applications

計劃編號: 98-2220-E-009-011- 執行期間:98 年 8 月~99 年 7 月

計劃主持人:交通大學電子系 鄭裕庭 教授 e-mail:ytcheng@mail.nctu.edu.tw

摘要

本計劃於三年執行期間共開發出四項應用於助聽器之技術，分別為低功率奈米複合線圈、仿醡醬草式音源定位麥克風，麥克風物理模型以及混合仿生式全域音源定位麥克風。在前兩年期間，我們開發出低功率喇叭的設計，利用奈米複合材料增強線圈磁性，經製程最佳化後，在銅鍍液中添加 2g/L 的奈米鎳粉，電鍍線寬為 200μm 之銅鎳複合線圈取代純銅線圈，可使喇叭在輸出同樣聲壓時節省 40%功率，以及仿酢漿草式麥克風，係利用低溫銅製程設計結合仿造酢漿草葉片及昆蟲聲源定位構造的電容式麥克風，以模擬方式將結構最佳化，並實驗量測得到位移量指向圖驗證，提供將聲源辨識微小化的可能性。此外，我們發展出浮動中央支撐平衡膜結構之仿生式麥克風模型在聲壓的梯度作用下之位移量預測模型，可針對結構靈敏度及剛性來設計調整最佳化，藉此，在第三年期間，我們開發出混合式仿生麥克風，經由理論分析及實驗證明，可以提供更好的靈敏度及方向性，優於傳統之中央支撐環結構，將可應用在助聽器元件之音源定位上。

Low power consumption microspeaker using Cu/Ni magnetic nanocomposite [1-3]

An electroplated Cu-Ni magnetic nanocomposite coil is developed and optimized for low-power electromagnetic microspeaker fabrication. Via the incorporation of Ni nano-particles into Cu matrix, the magnetic property can be effectively modified from diamagnetism to ferromagnetism without having drastic resistivity increase. Fig. 1 shows the M-H loop of Cu-Ni nanocomposites plated with different line structures in the baths with 2g/L Ni concentrations. It shows that Cu film has been modified from diamagnetism to ferromagnetism via the incorporation of Ni nano-particles. The power saving ratio determined by the trade-off between the electrical and magnetic properties of Cu-Ni nanocomposite can be calculated as follows:

$$\frac{P_{Composite}}{P_{Cu}} = \left(\frac{\mu_{r,Cu}}{\mu_{r,Composite}} \right)^2 \frac{k_{Cu}}{k_{Composite}} \qquad (1)$$

where $P_{Composite}/\mu_{r,Composite}/k_{Composite}$, $P_{Cu}/\mu_{r,Cu}/k_{Cu}$ are the power consumption, relative permeability, and conductivity of the coil made by Cu-Ni nanocomposite and pure Cu, respectively. By trading off the increase of magnetic flux density against the decrease of electrical conductivity of the actuated nanocomposite coils, better performance in terms of power saving can be found.

According to equation (1), the power saving can be estimated based on the measured electrical and magnetic properties. From the calculation, the optimal process condition, i.e. 200μm wide line structure electroplated in a bath with the Ni concentration of 2g/L, can have the highest power efficiency. According to SPL (Sound Pressure Level) versus input power normalized with the coil thickness due to the process variation in a frequency range from 1 to 6kHz as shown in Fig. 2, the composite coil can generate higher SPL than the Cu one under the same power input and averagely provide about 40% power saving than the Cu coil one for the same SPL output at 70dB. The inset of Fig. 2 shows the photograph of as-fabricated microspeaker.

In summary, we present a process optimization scheme for low-power electromagnetic microactuation using Cu-Ni nanocomposites. The optimal condition, i.e. 200μm wide inductive coil electroplated in a bath with the Ni concentration of 2g/L, can realize ~40% power saving of EM force driven speaker performed in a frequency range of 1 to 6kHz in comparison with the coil made of pure Cu for the same speaker design.

Oxalis-like microphone for sound source localization applications [4]

A micromachined microphone with oxalis-like electroplated copper sensing diaphragm is developed for sound source localization applications. The proposed microphone basically follows the concept which is a center-supported gimbal circular diaphragm structure proposed by Ono et al.[5-7]. However, instead of using a full circular diaphragm design, the oxalis-like leaf design combined with the employment of serpentine springs could resolve the problem due to the diaphragm disintegration which can make the sensing leaf more flexible to have larger deformation resulted by sound pressure. Meanwhile, the serpentine springs to connect the leaves with each other can ensure the whole sensing diaphragm vibrates in-phase and reversed-phase modes like the auditory organ of the parasitoid fly. Under 60dB SPL sound stimulation, about 70% of maximum displacement enhancement in a reversed-mode deformation can be obtained in comparison with the conventional design [8].

Fig. 3 shows the as-fabricated biomimetic microphone. Three copper layers are used as the top sensing diaphragm, supporting via, and the other sensing electrode at bottom, respectively. The inset of Fig. 3 is an enlarged view on the central gimbal region showing the fully released device structure. Fig. 4 shows the polar pattern of the normalized displacement of simulation and measured data by applying a pressure load 60dB SPL (0.02Pa) at 200Hz.

There is a large displacement discrepancy between the simulation and experimental data which could be resulted by applying incorrect sound pressure loading to the simulated structure. Therefore, a sound pressure gradient, which is about 0.062Pa/m close to the exact experimental setup, instead of uniform pressure load on the half of the sensing diaphragm is then applied for the analysis. The inset of Fig. 4 shows smaller displacement discrepancy between the simulation and experimental data. Although the discrepancy still exists, both results still provides qualitatively verification to the prediction of our ANSYS simulation.

In summary, a micromachined microphone with oxalis-like electroplated copper sensing diaphragm is presented for sound source localization applications. Experimental results verify the correctness of the simulation further indicating such a biomimetic microphone can indeed exhibit a better acoustic response for sound source localization.

Physical analytical model of center-supported gimbal circular diaphragm [9]

An analytical model in both views of material and dimensional characteristics is developed to well predict the net displacement and sound source localization of the biomimetic microphone based on a center-supported gimbal circular diaphragm. Mechanically and physically, by considering the angle of twist and deflection of a center-supported gimbal circular diaphragm caused by the time varying sound pressure gradient and gravity force, total displacements, Z(t), should be superposed:

$$Z(t)=\left\{\left[\frac{a^2-c^2}{2T^3aG}+\frac{8}{9\pi(a^2-c^2)E}\right]\cdot\int_{-a}^{a}P(r,t)\cdot\Delta\cdot r\cdot a\cos\varphi\,dr d\varphi\right\}+\frac{(a^2-c^2)\int_0^a m(r)g dr}{2Ta(T^2-W^2)E} \quad (2)$$

where P, Δ, g, W, m, T, G, E are sound pressure, gradient factor, gravity acceleration, width of beam, mass, thickness, shear modulus, and Young's modulus of material, respectively. Two cases are adopted for verifying the modeling analysis: 1.5μm thick diaphragm with a radius of 1500μm and 30μm thick diaphragm with a radius of 10.8mm, respectively. Fig. 5 presents the model validation for both cases by comparing model evaluations and experimental measurement demonstrated by Ono et al. [5-7]. 400 and 200Hz sinusoidal sound waves are chosen as sound source signals for the two cases, respectively. The results show good data matches in terms of displacement and related response with time variation. Slight mismatches might be due to the neglect of damping force. Therefore, based on the total displacements of center-supported gimbal circular diaphragm, design optimization could be first trade-off between structural sensitivity and rigidity by means of this analytical model.

In summary, an analytical model for prediction of biomimetic microphone mechanism on floating center-supported gimbal circular diaphragm is proposed. Excellence data match between the calculation and measurement result shows the accuracy of this model, and 50% improvement of the diaphragm displacement is predicted. By modifying the material dimensions and properties, the optimized structure will be found for sound source localization.

Hybrid Biomimetic Directional Microphone for the Full Space Sound Source Localization [10]

A hybrid biomimetic directional microphone with a central floating support is developed by hybridizing the supersensitive ears of the parasitoid fly with the flexibility of the clover stalk for the full space sound source localization. By introducing the mIIDpA, the mIPD, and the sensing region, the presented design with the state-of-the-art characteristics of mIIDpA 2.7dB/mm2 and mIPD 155° has shown a highly potential application for the directional microphone with full space sensitivity.

It has been being a challenge using a miniature microphone to realize sound source localization due to diminutive interaural level difference and interaural time difference. Several developed biomimetic MEMS microphones still exhibit several deficiencies, such as the structural sensitivity, rigidity and the process complexity with readout integration [5,11-13]. Among them, the biomimetic microphone proposed by Ono et al. has drawn lots of attention due to the characteristics of simple fabrication process, easy sensing circuit implementation, and good directional identification as well as signal sensing ability. However, the microphone using central pivot-supported (CP-S) designs [5], the asymmetrical beam structure, shown in Fig. 6 (a), would lead to an undesired deformation that might cause device failure or degradation of sensitive and directional abilities. In order to overcome this dilemma, we present a new symmetrical beam structure. By hybridizing the supersensitive ears of the parasitoid fly with the flexibility of the clover stalk, as shown in Fig. 6 (b), the structurally coupled mechanism of the central floating support reveals two unique design merits: (1) fourfold rotation axial symmetry of the central beams effectively compensates the undesired deformation due to gravity and residual stress for maintaining diaphragm rigidity, and (2) the central floating joint makes the sensing diaphragm more flexible for higher sound sensitivity and directivity.

By considering the equation of motion of the microphone diaphragm, the corresponding displacement in the steady state of the ipsi- (+) and contralateral (−) membranes can be expressed by the linear combination of the displacements of translational and rocking modes:

$$Z_{\pm} = \frac{P(t)\cdot\pi(a^2-c^2)}{m}\times \left\{\frac{\cos(\omega\tau/2)\sin(\omega t+\frac{\varphi_t}{2})}{\sqrt{(\omega_t^2-\omega^2)^2+(2\omega_t\eta_t\omega)^2}} \pm \frac{\sin(\omega\tau/2)\cos(\omega t+\frac{\varphi_r}{2})}{\sqrt{(\omega_r^2-\omega^2)^2+(2\omega_r\eta_r\omega)^2}}\right\} \quad (1)$$

where $P(t)$, a, c, m, τ, φ_t and φ_r, ω, ω_t and ω_r, and η_t and η_r are the sound pressure, the diaphragm radius, the radius of central support, the mass of the diaphragm, the time delay factor, the translational- and rocking-mode phases, the operating frequency, the translational- and rocking-mode resonant frequencies, and the translational- and rocking-mode damping ratios, respectively. Additionally, the performances of a biomimetic microphone can be also strictly compared using two mechanical indicators, the mechanical interaural intensity difference per area (mIIDpA) and the mechanical interaural phase difference (mIPD) [1], which can be obtained as follows:

$$\text{mIIDpA} = \left[20\log_{10}\frac{|Z_{ipsi}|}{|Z_{contra}|}\right] \Big/ \pi(a^2-c^2), \quad \text{mIPD} = \angle\frac{Z_{contra}}{Z_{ipsi}} \quad (2)$$

For instance, the ipsi- and contralateral membranes move in opposite directions with equal amplitudes must have the mIIDpA and mIPD with the values of near 0 dB/mm^2 and 180°, respectively. The presented hybrid design with the state-of-the-art characteristics of mIIDpA 2.7dB/mm^2 and mIPD 155° has shown highly potential applications for the directional microphone with full space sensitivity.

Meanwhile, for fairly comparison, two microphones with the hybrid and CP-S designs both having the same diameter and thickness are fabricated to validate device performance. Measured resonant frequencies of the hybrid and CP-S designs are about 10 and 12 KHz, respectively, close to the CoventorWare, as shown in Fig. 7 (a). Better directivity and larger net displacement in the polar plot shown Fig. 7 (b) reveal that the hybrid design has a superior ability in sound source localization, i.e. about 36% sensitivity and 34% directivity improvements in comparison with that of the CP-S design. Fig. 8 shows measured acoustic responses of the hybrid microphone applied with 80dB sound waves in frequency domain and it evidences that the hybrid design has well-performance at 200Hz with significant phase difference. Fig. 9 shows diaphragm displacement of the two kinds of microphones driven by a 80dB and 200Hz sinusoidal sound wave located at (r, θ, φ) = (24cm, 37°, 0°). The theoretical model for elaborating the dynamic response is likewise verified by experimental measurements depicted in Fig. 9. Excellence match between calculation and measurement results indicates the accuracy of presented model and about 30% net diaphragm displacement improvement.

In summary, we develop a hybrid biomimetic microphone with a central floating support. Better acoustic sensitivity and directivity can be realized theoretically and experimentally. The hybrid structure can not only inherit the advantages from conventional CP-S design, but also promote sound source localization sensitivity for MEMS microphones with a potential application for hearing aid devices.

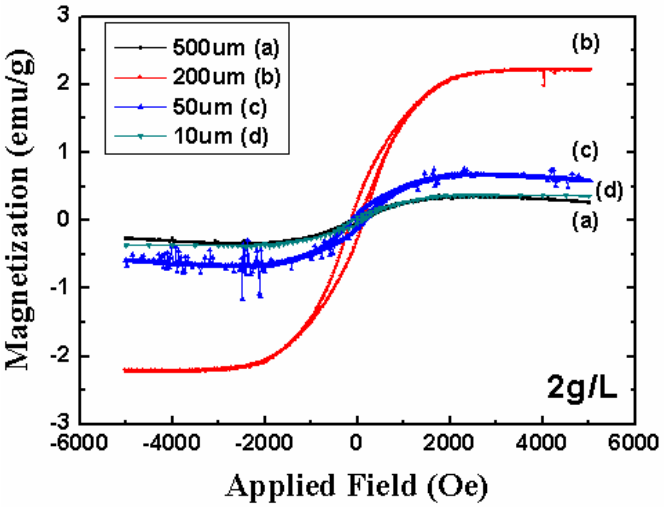

Fig. 1. SQUID results of Cu/Ni nanocomposites.

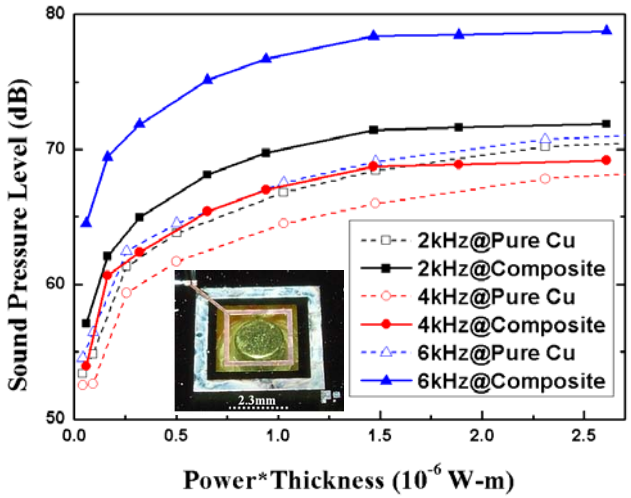

Fig. 2. Measured SPL spectrums of microspeakers made of pure Cu and Cu-Ni nanocomposite coils at 2, 4, and 6kHz, respectively.

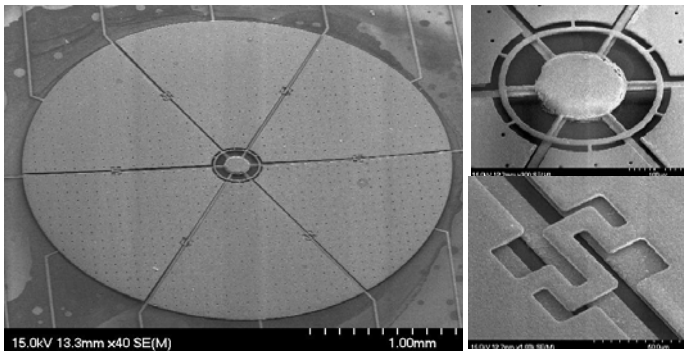

Fig. 3. The entire view of the as-fabricated microphone is photographed by SEM, and the enlarge view photographs focus on the serpentine spring and central gimbals region, respectively.

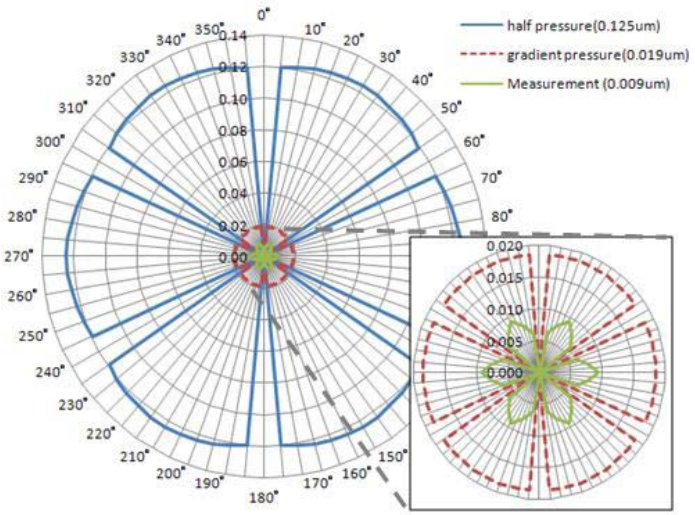

Fig. 4. The polar pattern of the net displacement of simulation and measured data by applying a pressure load 60dB SPL (0.02Pa) at 200Hz. The inset figure shows smaller displacement discrepancy between the simulation and experimental data while the sensing diaphragm is loaded with a pressure gradient.

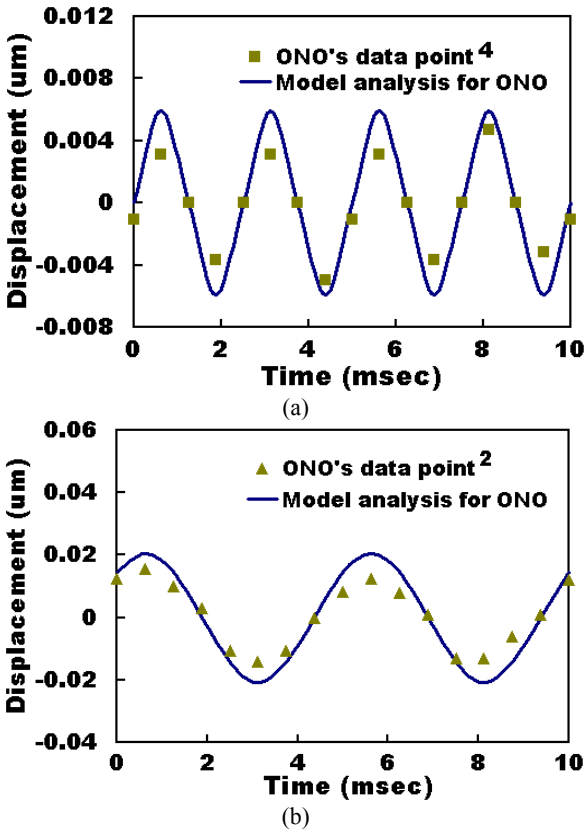

Fig. 5. Comparison between modeling analysis and experimental measurement demonstrated by Ono et al. (a) 400Hz and (b) 200Hz sinusoid sound waves with sufficient gradient factor applied for diaphragm with radius of 1500μm and 10.8mm, respectively.

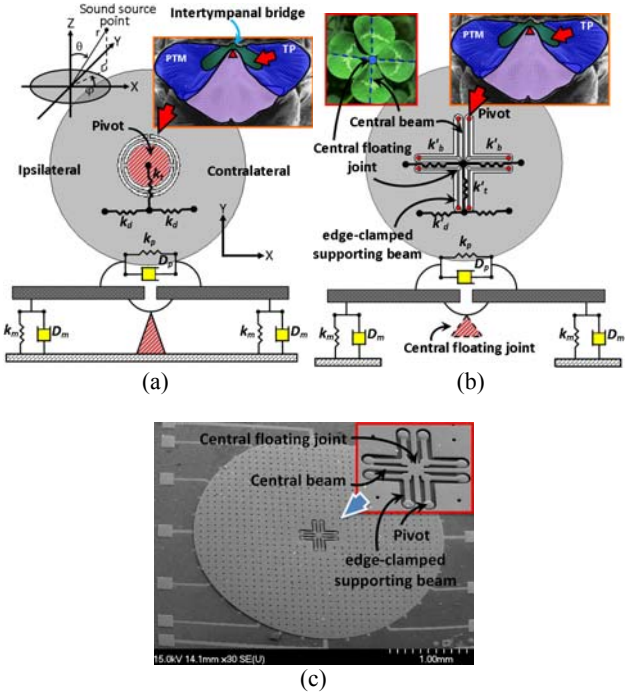

Fig. 6. (a) Schemes of the conventional CP-S design with coordinate parameters (r, θ, φ). (b) Scheme of the hybrid biomimetic microphone with central floating gimbal design. (c) The SEM photograph of the hybrid microphone.

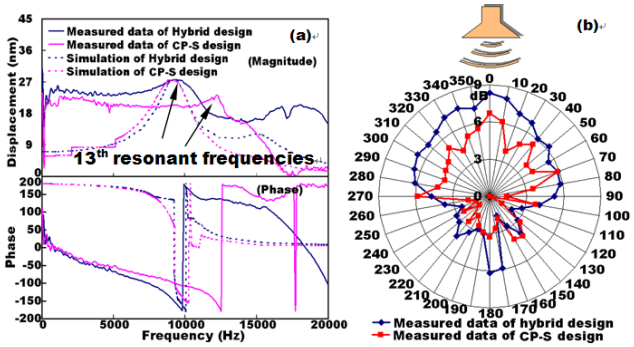

Fig. 7. Comparison of (a) the frequency spectrum and (b) the logarithmic polar patterns of net diaphragm displacement between hybrid and CP-S design.

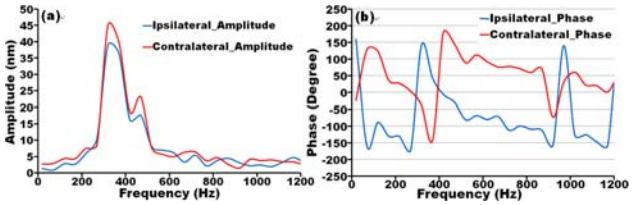

Fig. 8. Acoustic responses of hybrid design in frequency domain in terms of (a) amplitude, and (b) phase of ipsilateral and contralateral of diaphragm, respectively.

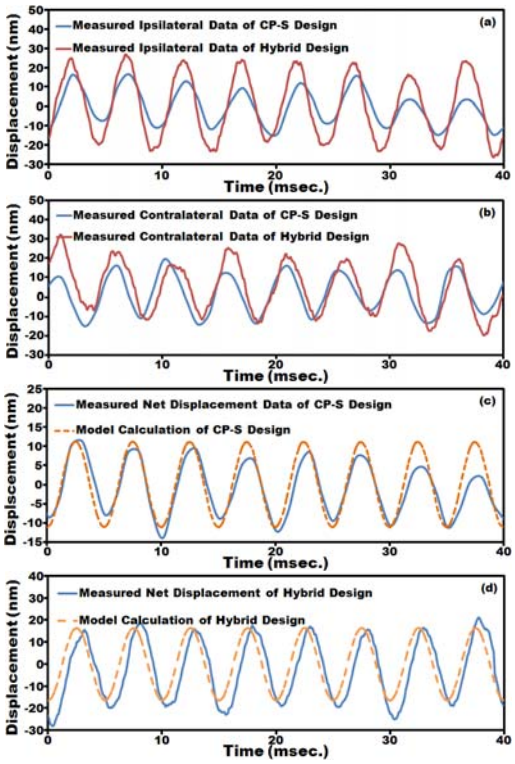

Fig. 9. Measured (a) ipsilateral and (b) contralateral results of hybrid and CP-S design, respectively. Comparison of model and net displacement are of (c) CP-S and (d) hybrid design, respectively.

Reference

[1] Yu-Wen Huang, Tzu-Yuan Chao, C. C. Chen, and Y. T. Cheng, "Power Consumption Reduction Scheme of Magnetic Microactuation Using Electroplated Cu-Ni Nanocomposite," *Appl. Phys. Lett.*, Vol. 90, 244105, 2007.

[2] Yu Wen Huang, Tzu-Yuan Chao, and Y.T. Cheng, "Synthesis and Device Fabrication of Cu-Ni Nanocomposite for Low Power Magnetic Microactuation," in *Proc. IEEE-NANO 2007*, Hong Kong, China, pp. 899-902, Aug. 2-5, 2007.

[3] Y. C. Chen, Wei-Ting Liu, Tzu-Yuan Chao, and Y. T. Cheng, "An Optimized Cu-Ni Nanocomposite Coil for Low-power Electromagnetic Microspeaker Fabrication," in *Proc. Transducers 2009*, Denver, Colorado, USA, Jun. 21-25, 2009.

[4] Y. C. Chen, C. C. Chen, Wen Hao Ching, and Y. T. Cheng, "Design and Fabrication of High Performance Biomimetic Microphone Using Oxalis-like Sensing Diaphragm for Sound Localization," in *Proc. APCOT2008*, Tainan, Taiwan, session 1B2-1, Jun. 22-25, 2008.

[5] N. Ono, A. Satio, and S. Ando, "Bio-mimicry Sound Source Localization with Gimbal Diaphragm", *T. IEE Japan*, vol. 123-E, pp. 92-97, 2003.

[6] N. Ono, A. Saito, and S. Ando, "Design and Experiments of Bio-mimicry Sound Source Localization Sensor with Gimbal-Supported Circular Diaphragm," in *Proc. Transducers'03*, pp.939-942, 2003.

[7] N. Ono, T. Arita, Y. Senjo, and S. Ando, "Directivity Steering Principle for Biomimicry Silicon Microphone," in *Proc. Transducers'05*, pp. 792-795, Jun. 2005.

[8] K. Yoo, J.-L. A. Yeh, N. C. Tien, C. Gibbons, Q. Su, W. Cui, and R. N. Miles, "Fabrication of a Biomimetic Corrugated Polysilicon Diaphragm with Attached Single Crystal Silicon Proof Masses," *Proc. Transducers'01*, pp. 130-133, Jun. 2001.

[9] C. C. Chen, Y. C. Chen, Keng-Yu Lin, and Y. T. Cheng, "A Novel Design and Analytical Model for Biomimetic Microphone with Floating Center-Supported Gimbal Circular Diaphragm," *第十三屆奈米工程暨微系統技術研討會*, 新竹, July 9-10, 2009.

[10]C. C. Chen, Y. C. Chen, K. Y. Lin, and Y. T. Cheng, "Hybrid Biomimetic Directional Microphone for the Full Space Sound Source Localization" in *Proc. Hilton Head Workshop 2010*, Jun. 6-10, 2010.

[11]H. J. Liu, M. Yu, and X. M. Zhang, "Biomimetic optical directional microphone with structurally coupled diaphragms," *Appl. Phys. Lett.*, 93, 243902-1, 2008.

[12]H. Liu, L. Currano, D. Gee, B. Yang, and M. Yu, "Fly-Ear Inspired Acoustic Sensors for Gunshot Localization," in *Proc. SPIE*, 7321, 73210A-1, May. 4, 2009.

[13]W. Cui, B. Bicen, N. Hall, S. A. Jones, F. L. Degertekin, and R. N. Miles, "Optical Sensing Inadirectional Memsmicrophone Inspired by the Ears of the Parasitoid Fly, Ormia Ochracea," in *Proc. MEMS2006*, pp. 614-617, 2006.

Hilton Head 2010 Review Report

2010 年美國傳感學會所舉辦之第十五屆微感測制動元件暨系統會議於六月六日假美國南卡州希爾頓頭島舉行。四天會期共包含三篇大會邀請演講、26 場口頭報告、以及87篇海報報告。內容涵蓋奈米技術應用於射頻、光學、生物、能源、微流體系統、感測與致動器之製作與微系統封裝之相關設計、製造技術之研發成果報告。由於所發表之文章乃由271篇稿件節選而出，在~42%接受率的選取條件之下，涵蓋領域雖廣，文章內容極佳且具代表性。此外本會僅限北美地需相關研究人員以及會友得以參加，是故台灣於此次會議僅有敝人一篇研究報告發表。

從本人觀點而言，下列幾篇報告相當有趣且及其重要：首先為大會邀請之演講，InvenSense Dr. Seeger報告近年來InvenSense於微機電式慣性感測器與平台之相關發展，強調六軸慣性感測器之相關設計與製造技術所面臨之挑戰與如何於三維空間中有效提升慣性感測器之靈敏度與數位訊號輸出，並以真空封裝製程限制下實現低價且高製造良率之六軸慣性感測器以及未來慣性感測平台發展於消費性電子產品如4G i-phone等之重要性。基本上本演講已揭露MEMS產業蓬勃發展時代之來臨。 在致動器設計方面今年加州理工學院提出以仿尺蠖運動模式以及電化學反應驅動矽膠氣球進而控制制動夾具原理，設計出可精準控制神經探針之致動器，由於該制動器可操作於低電壓與低電流之操作範圍下使得該系統在100μW驅動功率下可有25 ~75μm之位移非常適用於生物體內之操作。而在射頻微機電元件研究上，今年則以元件製程開發之論文教引人注目，以加州大學爾灣分校所提出以矽基板與玻璃晶圓氣密接合為基礎，藉由密封氣體受熱膨脹之機制將接合之玻璃基材於高溫下形成球狀結構，由於球狀對稱之3-D結構以及與基板間之接觸面積較小，將使得以此結構作為之共震器有著具有較高之品質因素表現。該製程亦與密西根大學所提之Glass-in-Silicon之技術有異曲同工之妙，藉由高溫玻璃融熔回流之特性，將一經過微加工處理之矽晶圓內部填充玻璃並經由晶圓磨薄技術完成Glass-in-Silicon基板以利後續微系統之製作。應形成金屬矽化合物並造成結構體積微縮，此微縮現象將行形成於nm尺寸大小之結構間隙。

最後以加州大學洛杉磯分校所提出以光催化反應機制建構一濕式電蝕刻槽以取代傳統乾式深度電漿蝕刻(DRIE)方式，此舉將可有效降低製造成本，此外該技術可實現 1:60 之深寬比且不規則形狀之 VIAS 包含條狀、鋸齒狀與蚊香狀等，對於 3D-IC 中的 TSV 製造成本降低亦具影響力。微感測元件與製造技術是一種工具和方法，提供各領域遭遇關鍵瓶頸時的解決之道，甚或提供微小化與大量製造之可行性，是一門跨領域與高度整合之學門，每年都有非常嶄新之研究成果發表，參加該會議除可增廣見聞，有助自身研究之外，更可與北美一流學者互動，增加國際合作之機會，因此此次會議本人收穫實屬良多。

Yu-Ting Cheng,
Department of Electronics Engineering,
National Chiao Tung University.

HYBRID BIOMIMETIC DIRECTIONAL MICROPHONE FOR THE FULL SPACE SOUND SOURCE LOCALIZATION

C. C. Chen, Y. C. Chen, Keng-Yu Lin, and Y. T. Cheng*
Microsystems Integration Laboratory, Department of Electronics Engineering & Institute of Electronics,
National Chiao Tung University, Hsinchu, Taiwan, ROC.

ABSTRACT

The paper presents a hybrid biomimetic directional microphone with a central floating pivot support by hybridizing the supersensitive ears of the parasitoid fly with the flexibility of the clover stalk. By introducing the mIIDpA, the mIPD, and the sensing region, the presented design with the state-of-the-art characteristics of mIIDpA 2.7dB/mm^2 and mIPD 155° has shown a highly potential application for the sound source localization with full space sensitivity. Excellence match between theoretical calculation and measurement results indicates the accuracy of the presented model and about 30% net diaphragm displacement improvement.

INTRODUCTION

It has been a challenge using a miniature microphone to realize sound source localization due to diminutive interaural level difference and time difference [1]. Several developed biomimetic MEMS microphones still exhibited several deficiencies, such as the trade-off of structural sensitivity and rigidity and the increase of process complexity with optical readout integration [1,2,4]. Among them, the biomimetic microphone using a central pivot-supported (CP-S) design [3] has drawn lots of attention due to the characteristics of simple fabrication process, easy sensing circuit implementation, and good directional identification as well as signal sensing ability. However, the asymmetrical beam structure, shown in Fig. 1 (a), would lead to an undesired deformation that might cause device failure or the degradation of device sensitive and directional abilities. In order to overcome this dilemma, we present a new symmetrical beam structure. By hybridizing the supersensitive ears of the parasitoid fly with the flexibility of the clover stalk, as shown in Fig. 1 (b) and (c), the structurally coupled mechanism of the central floating support reveals two unique design merits: (1) fourfold rotation axial symmetry of the central beams effectively compensates the undesired deformation due to the gravity and the residual stresses for maintaining diaphragm rigidity, and (2) the central floating joint makes the sensing diaphragm more flexible for higher sound sensitivity and directivity.

For fair comparison, two microphones with the hybrid and CP-S designs both having the same structure parameters listed in Table 1 are fabricated using a three-layer copper electroplating process [5] respectively to validate device performance. Measured resonant frequencies of the hybrid and CP-S designs are about 10 and 12 KHz, respectively, close to the CoventorWare simulation [6] shown in Fig. 2 (a). Better directivity and larger net displacement in the polar plot shown in Fig. 2 (b) reveal that the hybrid design has a superior ability in sound source localization, i.e. about 36% sensitivity and 34% directivity improvements in comparison with that of the CP-S design. Figure 3 shows measured acoustic responses of the hybrid microphone applied with 80dB sound waves in frequency domain and it evidences that the hybrid design has well-performance at 200Hz with significant phase difference. Figure 4 shows the diaphragm displacements of the two kinds of microphones driven by a 80dB and 200Hz sinusoidal sound wave located at (r, θ, φ) = (24cm, 37°, 0°).

Meanwhile, by considering the motion equation of the microphone diaphragm, the corresponding displacement in the steady state of the ipsi- (+) and contralateral (−) membranes can

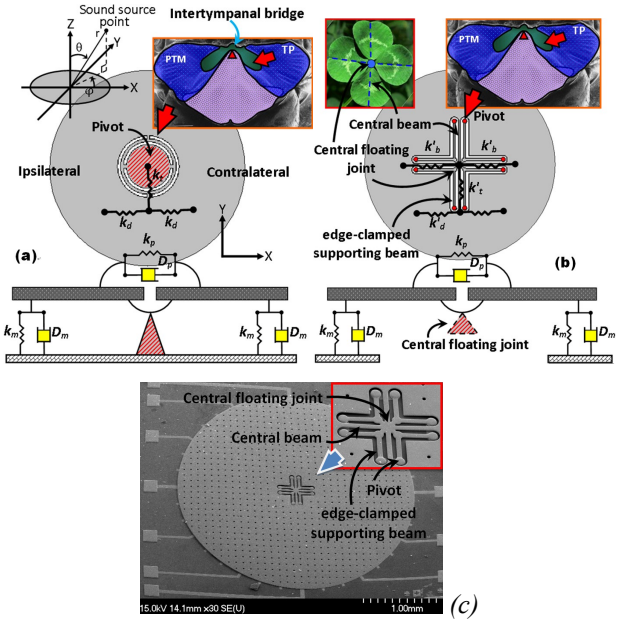

Figure 1: (a) Schemes of the conventional CP-S design with coordinate parameters (r, θ, φ). (b) Scheme of the hybrid biomimetic microphone with central floating gimbal design. (c) The SEM photograph of the hybrid microphone.

be expressed by the linear combination of the displacements of translational and rocking modes:

$$Z_{\pm} = \frac{P(t)\cdot\pi(a^2-c^2)}{m}\times \left\{ \frac{\cos(\omega\tau/2)\sin(\omega t+\frac{\varphi_t}{2})}{\sqrt{(\omega_t^2-\omega^2)^2+(2\omega_t\eta_t\omega)^2}} \pm \frac{\sin(\omega\tau/2)\cos(\omega t+\frac{\varphi_r}{2})}{\sqrt{(\omega_r^2-\omega^2)^2+(2\omega_r\eta_r\omega)^2}} \right\} \quad (1)$$

where $P(t)$, a, c, m, τ, φ_t and φ_r, ω, ω_t and ω_r, and η_t and η_r are the sound pressure, the diaphragm radius, the radius of central support, the mass of the diaphragm, the time delay factor, the translational- and rocking-mode phases, the operating frequency, the translational- and rocking-mode resonant frequencies, and the translational- and rocking-mode damping ratios, respectively. The theoretical model for elaborating the dynamic response is likewise verified by experimental measurements depicted in Fig. 4. Excellence match between calculation and measurement results indicates the accuracy of presented model and about 30% net diaphragm displacement improvement. Additionally, the performances of a biomimetic microphone can be also strictly compared using two mechanical indicators, the mechanical interaural intensity difference per area (mIIDpA) and the mechanical interaural phase difference (mIPD) [1], which can be obtained as follows:

$$\text{mIIDpA} = \left[20\log_{10}\frac{|Z_{ipsi}|}{|Z_{contra}|} \right] \Big/ \pi(a^2-c^2), \quad \text{mIPD} = \angle\frac{Z_{contra}}{Z_{ipsi}} \quad (2)$$

Table 1: Dimension parameters of the hybrid and CP-S design

Hybrid design	
Radius of diaphragm (*a*)	1500μm
Thickness of diaphragm (*T*)	5μm
Length of edge-clamped supporting beam (*L*)	250μm
Length of central beam (*L*)	250μm
Width of beam (*W*)	15μm
Spacing between beams	15μm
CP-S design	
Radius of diaphragm (*a*)	1500μm
Thickness of diaphragm (*T*)	5μm
Radius of CP region (*c*)	225μm
Radius of ring	270μm
Width of ring	30μm
Length of beam (*L*)	30μm
Width of beam (*W*)	30μm

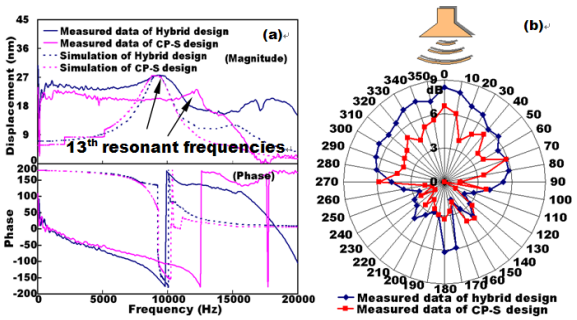

Figure 2: Comparison of (a) the frequency spectrum and (b) the logarithmic polar patterns of net diaphragm displacements between the hybrid and CP-S design.

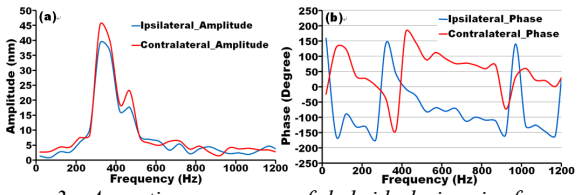

Figure 3: Acoustic responses of hybrid design in frequency domain in terms of (a) amplitudes and (b) phases of ipsilateral and contralateral of diaphragm, respectively.

For instance, the ipsi- and contralateral membranes move in opposite directions with equal amplitudes must have the mIIDpA and mIPD with the values of near 0 dB/mm^2 and 180°, respectively. Table 2 shows the comparisons in terms of nature frequencies and mechanical performances between the parasitoid fly [2], the conventional designs [1,3,4] and the new structure. The presented hybrid design with the state-of-the-art characteristics of mIIDpA 2.7dB/mm^2 and mIPD 155° has shown a highly potential application for the sound source localization with full space sensitivity.

In summary, we develop a hybrid biomimetic microphone with a central floating pivot support. Better acoustic sensitivity and directivity can be realized theoretically and experimentally. The hybrid structure can not only inherit the advantages from conventional CP-S design, but also promote sound source localization sensitivity for MEMS microphones with a potential application for hearing aid devices [1].

REFERENCES

[1] H. J. Liu, M. Yu, and X. M. Zhang, "Biomimetic optical directional microphone with structurally coupled diaphragms," Applied Physics Letters, 93, 243902-1 (2008).

[2] H. Liu, L. Currano, D. Gee, B. Yang, and M. Yu, "Fly-Ear Inspired Acoustic Sensors for Gunshot Localization," Proc. of SPIE, 7321, 73210A-1 (2009).

[3] N. Ono, A.Satio, and S. Ando, "Design and experiments of bio-mimicry sound source localization sensor with gimbal-supported circular diaphragm," Conference on Solid State Sensors, Actuators and Microsystems, Boston (2003), pp.935-938.

[4] W. Cui, B. Bicen, N. Hall, S. A. Jones, F. L. Degertekin, and R. N. Miles, "Optical Sensing Inadirectional Memsmicrophone Inspired by the Ears of the Parasitoid Fly, Ormia Ochracea," Proc. IEEE MEMS, 614 (2006).

[5] Y. C. Chen, C. C. Chen, Wen Hao Ching and Y. T. Cheng, "Design and Fabrication of High Performance Biomimetic Microphone Using Oxalis-Like Sensing Diaphragm for Sound Localization," APCOT Digest, 1B2-1(2008).

[6] CoventorWare, http://www.coventor.com/, version 2008.

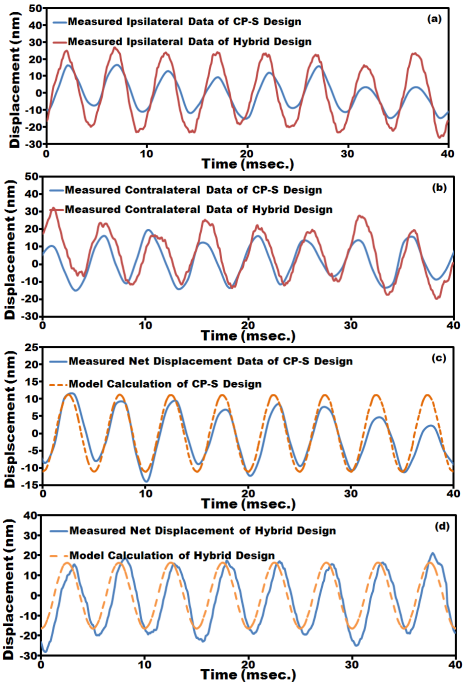

Figure 4: Measured (a) ipsilateral and (b) contralateral results of hybrid and CP-S design, respectively. Comparison of model and net displacement are of (c) CP-S and (d) hybrid design, respectively.

Table 2: Comparisons in terms of nature frequencies and mechanical performances.

Comparison	First translational mode frequency	First rocking mode frequency	mIIDpA (dB/ mm^2)	mIPD (deg)	Full space sensing
Parasitoid fly [2]	31KHz	7.1KHz	10.0	80	Yes
Ref. [1]	2.0KHz	1.2KHz	0.5	95	No
Ref. [3]	0.7KHz*	0.2KHz*	2.7	135	Yes
Ref. [4]	2.0KHz	X	10.5	X	No
New design	1.8KHz*	0.7KHz*	2.7	155	Yes

* : theoretical derivation; X: not available

CONTACT

*C. C. Chen, Tel: +886-3-5712121 #54223; gettgod.ee92g@nctu.edu.tw

國科會補助計畫衍生研發成果推廣資料表

日期 2010年10月27日

國科會補助計畫	計畫名稱: 子計畫七：微機電式聲學元件暨助聽器異質整合(3/3) 計畫主持人: 鄭裕庭 計畫編號: 98 -2220-E -009 -011 - 學門領域: 晶片科技計畫--整合型學術研		
研發成果名稱	(中文) 低功率消耗磁性奈米複合材料微型喇叭		
	(英文) Low power consumption microspeaker using magnetic nanocomposite		
成果歸屬機構	國立交通大學	發明人 (創作人)	鄭裕庭,陳永昌,陳健璋
技術說明	(中文)微機電式微型喇叭通常設計是以通有電流之電感性微型線圈在磁場下產生的電磁力來驅動。由電磁力驅動之微型喇叭能提供較大的輸出力與較低驅動電壓。因此，它會更容易勝任處理低功耗的問題。基於本研究羣先前的研究成果，利用銅鎳奈米複合材料可使電力消耗減少約9%，然而由於其具有較大的電阻率而無法達到最好之狀況。因此，對於低功率消耗之應用此技術仍然需要最佳化設計。藉由權衡磁通密度增加與降低奈米複合材料驅動線圈之電阻率，可達成更好的節省功率特性。一個寬為200μm的複合材料線圈在添加了2g/L鎳奈米粉末的鹼性非氰化物銅電鍍浴中電鍍，在頻率為1至6kHz的範圍內，奈米複合材料喇叭可較相同設計之純銅喇叭減少大約40%之功率消耗。		
	(英文)MEMS microspeaker are typically designed with an inductive microcoil driven by an electrical current under a magnetic field to generate electromagnetic force (EMF). The microspeaker operating with EMF can provide larger output force with low driving voltage and be easier to fit for the low power consumption issue. Based on our previous achievement and by trading off the increase of magnetic flux density against the decrease of electrical conductivity of the actuated nanocomposite coils, better performance in terms of power saving can be found. A 200μm wide composite coil plated in an alkaline noncyanide copper based bath that is added with 2g/L of Ni nanopowders can realize ~40% power saving of the speaker performed in a frequency range of 1 to 6kHz as compared with the coil made of pure		
產業別	電機及電子機械器材業，醫療器材製造業		
技術/產品應用範圍	Hearing aids, MEMS, Personal protable devices		
技術移轉可行性及預期效益	The technology can be widely utilized in electromagnetic based actuators which require low-power function.		

註：本項研發成果若尚未申請專利，請勿揭露可申請專利之主要內容。

98 年度專題研究計畫研究成果彙整表

計畫主持人：鄭裕庭	計畫編號：98-2220-E-009-011-
計畫名稱：助聽器晶片及系統--子計畫七：微機電式聲學元件暨助聽器異質整合(3/3)	

成果項目			量化			單位	備註（質化說明：如數個計畫共同成果、成果列為該期刊之封面故事...等）
			實際已達成數（被接受或已發表）	預期總達成數(含實際已達成數)	本計畫實際貢獻百分比		
國內	論文著作	期刊論文	0	0	100%	篇	
		研究報告/技術報告	0	0	100%		
		研討會論文	1	0	100%		
		專書	0	0	100%		
	專利	申請中件數	1	0	100%	件	
		已獲得件數	0	0	100%		
	技術移轉	件數	0	0	100%	件	
		權利金	0	0	100%	千元	
	參與計畫人力（本國籍）	碩士生	2	0	100%	人次	
		博士生	2	0	100%		
		博士後研究員	0	0	100%		
		專任助理	0	0	100%		
國外	論文著作	期刊論文	1	0	100%	篇	
		研究報告/技術報告	0	0	100%		
		研討會論文	1	0	100%		
		專書	0	0	100%	章/本	
	專利	申請中件數	1	0	100%	件	
		已獲得件數	0	0	100%		
	技術移轉	件數	0	0	100%	件	
		權利金	0	0	100%	千元	
	參與計畫人力（外國籍）	碩士生	0	0	100%	人次	
		博士生	0	0	100%		
		博士後研究員	0	0	100%		
		專任助理	0	0	100%		

其他成果 (無法以量化表達之成果如辦理學術活動、獲得獎項、重要國際合作、研究成果國際影響力及其他協助產業技術發展之具體效益事項等，請以文字敘述填列。)	無

	成果項目	量化	名稱或內容性質簡述
科教處計畫加填項目	測驗工具(含質性與量性)	0	
	課程/模組	0	
	電腦及網路系統或工具	0	
	教材	0	
	舉辦之活動/競賽	0	
	研討會/工作坊	0	
	電子報、網站	0	
	計畫成果推廣之參與（閱聽）人數	0	

國科會補助專題研究計畫成果報告自評表

請就研究內容與原計畫相符程度、達成預期目標情況、研究成果之學術或應用價值（簡要敘述成果所代表之意義、價值、影響或進一步發展之可能性）、是否適合在學術期刊發表或申請專利、主要發現或其他有關價值等，作一綜合評估。

1. 請就研究內容與原計畫相符程度、達成預期目標情況作一綜合評估

■達成目標

□未達成目標（請說明，以 100 字為限）

□實驗失敗

□因故實驗中斷

□其他原因

說明：

2. 研究成果在學術期刊發表或申請專利等情形：

論文：■已發表 □未發表之文稿 □撰寫中 □無

專利：□已獲得 ■申請中 □無

技轉：□已技轉 □洽談中 ■無

其他：(以 100 字為限)

3. 請依學術成就、技術創新、社會影響等方面，評估研究成果之學術或應用價值（簡要敘述成果所代表之意義、價值、影響或進一步發展之可能性）(以 500 字為限)

微機電式聲學元件開發為本子計劃之主要研究要務，技術創新上即成功利用奈米複合複合材料調變導電線圈特性，藉由權衡磁通密度增加與降低奈米複合材料驅動線圈之電阻率可使微型電感性喇叭電力消耗減少約 40%，因此，對於低功率消耗之感測與致動器應用需求上，此技術將可廣泛達成更好的節省功率特性。此外我們亦發展出浮動中央支撐平衡膜結構之仿生式麥克風在聲壓的梯度作用下，可以提供更好的靈敏度及方向性，將可應用在助聽器元件之音源定位上。